

Geophysical Research Letters*



RESEARCH LETTER

10.1029/2025GL117567

Key Points:

- Flux tube integrals of Jupiter's magnetosphere are calculated from in situ Juno data to diagnose the system's global stability
- On average, Jupiter's middle magnetosphere is stable for interchange motion based on the criteria from Southwood and Kivelson (1987, https://doi.org/10.1029/ ja092ia01p00109)
- For injection events, plasma flow observations are consistent with the interchange instability criteria prediction

Supporting Information:

Supporting Information may be found in the online version of this article.

Correspondence to:

J.-Z. Wang, jiwa1124@colorado.edu; jian-zhao.wang@lasp.colorado.edu

Citation:

Wang, J.-Z., Bagenal, F., Wing, S., Delamere, P. A., Ma, X., Wilson, R. J., et al. (2025). Flux tube properties and interchange instabilities in Jupiter's middle magnetosphere. *Geophysical Research Letters*, 52, e2025GL117567. https://doi.org/10.1029/2025GL117567

Received 11 JUN 2025 Accepted 23 OCT 2025

© 2025. The Author(s). This is an open access article under the terms of the Creative Commons Attribution License, which permits use, distribution and reproduction in any medium, provided the original work is properly cited.

Flux Tube Properties and Interchange Instabilities in Jupiter's Middle Magnetosphere

Jian-Zhao Wang^{1,2}, Fran Bagenal¹, Simon Wing³, Peter A. Delamere⁴, Xuanye Ma⁵, Robert J. Wilson¹, Robert W. Ebert^{6,7}, Philip W. Valek⁶, Frederic Allegrini^{6,7}, Vincent Dols¹, Licia C. Ray⁸, Chynna Spitler⁴, George Clark³, and Barry H. Mauk³

¹Laboratory for Atmospheric and Space Physics, University of Colorado Boulder, Boulder, CO, USA, ²Department of Astrophysical and Planetary Sciences, University of Colorado Boulder, Boulder, CO, USA, ³Applied Physics Laboratory, The Johns Hopkins University, Laurel, MD, USA, ⁴Geophysical Institute, University of Alaska Fairbanks, Fairbanks, AK, USA, ⁵Physical Sciences Department, Embry-Riddle Aeronautical University, Daytona Beach, FL, USA, ⁶Southwest Research Institute, San Antonio, TX, USA, ⁷Department of Physics and Astronomy, University of Texas at San Antonio, San Antonio, TX, USA, ⁸Physics Department, Lancaster University, Lancaster, UK

Abstract In Jupiter's magnetosphere, the outward transport of Io-genic plasma and the planetward injection of energetic particles are facilitated by flux tube interchange motion driven by centrifugal instabilities. Flux tube content and entropy are two competing key quantities that determine the behavior of the system. In this study, we first review the centrifugal force driven dynamics in different regions. Benefiting from Juno's high-quality in situ data in the off-equatorial region, we then analyze the flux tube integrals and interchange instability criteria between M-shells 13 and 40 using numerical integration. On average, the entropy term dominates the system, resulting in a generally stable system for interchange motion. Finally, we investigate an injection event, in which predictions from the criteria align with the observed flow direction. This study illustrates the overall stability of the system with small-scale, intermittent dynamic phenomena.

Plain Language Summary Jupiter's magnetosphere is filled with plasma primarily sourced from Io's escaping atmosphere. Due to the planet's rapid rotation and the high loading rate of plasma from Io, the structure and dynamics of the magnetosphere are strongly influenced by centrifugal forces. The plasma is confined within flux tubes, which are bundles of magnetic field lines that guide and contain plasma through space. Radial plasma transport is mainly facilitated by flux tube interchange, a process in which two neighboring flux tubes exchange positions. The stability of the magnetosphere against such interchange motion depends on the radial distributions of two competing properties: the total plasma content and the internal energy density (or entropy) of each flux tube. In Jupiter's middle magnetosphere, flux tube content decreases with increasing radial distance, driving outward plasma transport and destabilizing the system. In contrast, flux tube entropy increases with distance, exerting a net inward force on the plasma and promoting stability. When considered together, the entropy term typically dominates on average, resulting in a system that is generally stable against interchange motion.

1. Introduction

1.1. Centrifugal Force Driven Dynamics

Centrifugal forces and rotation-driven processes play significant roles in structuring Jupiter's magnetosphere and governing its dynamics (Kivelson & Southwood, 2005). Neutrals from Io's escaping atmosphere are ionized and trapped by Jupiter's strong magnetic field (reviewed by Bagenal and Dols (2020)). The plasma is confined near the equatorial region and transported outward in response to rotational stresses, forming a thin plasma disk (reviewed by Bagenal and Delamere (2011)). In the inner magnetosphere, plasma transport is facilitated by flux tube interchange, a spontaneously triggered process in which an inner flux tube with higher mass replaces a neighboring outer tube with lower mass (Hill, 1976). Whole flux tube interchange (top row of Figure 1) involves the simultaneous convection of two flux tubes in both the equatorial region and at their respective ionospheric footprints. However, whole flux tube interchange is difficult to perform because the equatorial region is more unstable to interchange motion than the off-equatorial region. Alternatively, localized interchange (second row of Figure 1) is considered a more plausible mechanism, in which flux tubes are twisted and stretched locally due to

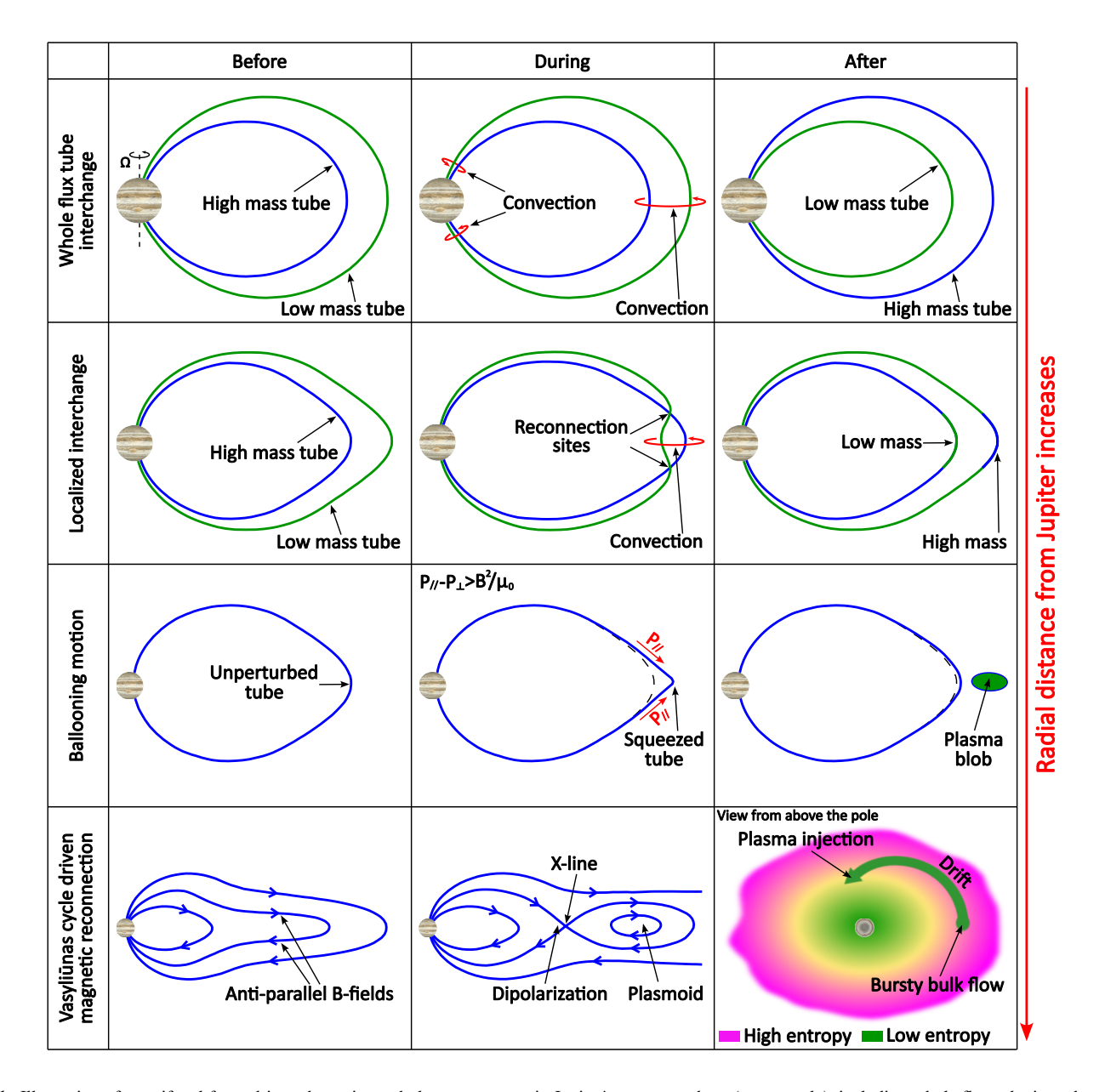


Figure 1. Illustration of centrifugal force driven dynamics and plasma transport in Jupiter's magnetosphere (not to scale), including whole flux tube interchange, localized interchange, ballooning motion, and Vasyliūnas cycle driven reconnection. Each mechanism is depicted in three stages: before, during, and after.

the equatorial convection pattern (Ma et al., 2019). Consequently, a pair of off-equatorial reconnection sites may be triggered if the shear angle between the two tubes becomes sufficiently large (Ma et al., 2016).

Flux tubes are increasingly stretched radially as the radial distance increases, and particles gain parallel energy through bounce motion, leading to pressure anisotropy in the rotating plasma (Paranicas et al., 1991; Vogt et al., 2014). The firehose instability occurs when the parallel pressure exceeds the perpendicular pressure by more than the magnetic pressure (i.e., $p_{\parallel}-p_{\perp}>B^2/\mu_0$). The Alfvén wave speed is reduced and may become unstable (Abraham-Shrauner, 1967), preventing fluctuations from propagating back to Jupiter. Plasma undergoes ballooning motion (third row of Figure 1), where the flux tube is squeezed by the increasing parallel pressure and bulges outward due to centrifugal force (Kivelson & Southwood, 2005). Eventually, the flux tube loses its integrity and blows open with eruptions of outward-moving plasma blobs (André & Lemaire, 2006; Wang, Bagenal, Wilson, Delamere, Ebert, et al., 2025). In the outer magnetosphere, further stretching of flux tubes occurs as plasma moves outward while remaining frozen to the magnetic field. The merging of oppositely directed

WANG ET AL. 2 of 11



magnetic field lines leads to magnetic reconnection, as part of the Vasyliūnas cycle (Vasyliūnas, 1983) (bottom row of Figure 1). Reconnection releases outward-moving plasmoids and inward-moving dipolarization fronts, producing plasma jets known as bursty bulk flows (Louarn et al., 2015; Woch et al., 1999). The flows have lower internal plasma energy density (or entropy) than the surrounding plasma in the tail. To reach equilibrium, they are injected inward with energy-time dispersion (Mauk et al., 2005) until they encounter plasma of similar entropy and a new equilibrium is established (Wolf et al., 2009). Theoretically, all these mechanisms contribute to the outward transport and loss of Io-genic plasma, although their relative significance remains an open question.

1.2. Flux Tube Integrals and Instability Criteria

In a rapidly rotating magnetosphere, plasma transport is governed by two flux tube integrals: flux tube content (N) and flux tube entropy (S). N measures the total amount of plasma confined within a magnetic flux tube, while S, a conserved quantity under adiabatic motion, helps explain stability, injection, and interchange dynamics (Birn et al., 2009; Johnson & Wing, 2009; Wing & Johnson, 2009, 2010). Continuous plasma production near Io creates a negative flux tube content gradient, driving outward motion via centrifugal forces (Bagenal & Delamere, 2011). Conversely, increasing flux tube entropy with distance, as suprathermal ions dominate plasma pressure in the outer region, produces a net inward force (Delamere et al., 2015; Wing et al., 2024). Gold (1959) demonstrated that flux tubes are unstable if entropy decreases with radial distance under a dipolar field assumption. Hill (1976) highlighted the role of rotation, showing that interchange motion is unstable if flux tube content is a decreasing function of distance. Southwood and Kivelson (1987) developed a generalized interchange model, free from restrictions on magnetic field geometry, that incorporates both flux tube content and entropy, and highlights the competing nature of these two parameters. André and Ferrière (2004) derived the dispersion relation for a lowfrequency mode associated with interchange instabilities and obtained a criterion describing instabilities triggered by thermal pressure anisotropies and stratification. Notably, both Southwood and Kivelson (1987) and André and Ferrière (2004) reduce to the Gold (1959) criteria when only curvature forces are considered and to the Hill (1976) criteria when only centrifugal forces are considered.

Interchange instability in fast-rotating magnetospheres has been investigated using in situ observations. At Saturn, Sittler et al. (2008) reported that flux tube content peaks at near 6 Saturn radii, marking the main plasma source region, and decreases outside this location, suggesting that the plasma disk is unstable to centrifugal interchange. As direct evidence of interchange motion, plasma is transported outward, with radial velocity increasing with radial distance in Saturn's inner magnetosphere (Sittler et al., 2006). Detached cold, dense plasma blobs from the plasma disk are observed and may represent outward-convected remnants of flux tubes after breaking open, resembling the ballooning mode (Goertz, 1983). Ma et al. (2019) found that plasma entropy increases between 6 and 20 Saturn radii, indicating non-adiabatic heating (or cooling) during outward (or inward) plasma transport. Wing et al. (2022) analyzed seven injection events, showing that plasma entropy limits inward transport by balancing centrifugal force between 8.5 and 11 Saturn radii, which explains the rarity of injections within 6 Saturn radii (Azari et al., 2018). At Jupiter, Mauk et al. (1998) reported the radial gradient of plasma entropy in Io's plasma torus and concluded that the hot plasma population impeded radial plasma transport. Kivelson et al. (1997) reported short-duration interchange events around Io with 1–2% changes of the background magnetic field, implying that interchange can occur without significant reconfiguration. Correspondingly, both small- and large-scale intermittent structures in plasma density are observed, indicating interchange motion that drives the outward transport of Io-genic plasma (McNutt et al., 1981; Scudder et al., 1981; Sittler & Strobel, 1987). Russell et al. (2005) conducted a statistical survey of plasma-depleted flux tubes characterized by abrupt increases in magnetic field magnitude, suggesting that two distinct flux tubes were encountered within a narrow channel. Accompanied by enhancements in plasma waves and pitch angle anisotropy (Bolton et al., 1997; Thorne et al., 1997), these events are consistent with the concept of plasma injection, in which rapid inward transport occurs.

Prior to Juno, plasma observations in Jupiter's magnetosphere were largely limited to the equatorial region, necessitating model-based extrapolations of flux tube behavior. As Jupiter's first polar orbiter, Juno provides high-quality plasma observations in the off-equatorial regions. In this study, we aim to investigate the interchange instability in Jupiter's magnetosphere from two perspectives: the average plasma conditions and a case study of an injection event.

WANG ET AL. 3 of 11



2. Data and Method

2.1. Juno's In Situ Data

The Juno mission measures thermal plasma by JADE (Jovian Auroral Distributions Experiment) (McComas et al., 2017). JADE consists of two electron sensors (JADE-Es) and one ion sensor (JADE-I), which incorporates an electrostatic analyzer (ESA) and a time-of-flight (TOF) mass spectrometer. The ESA measures the energy-percharge ratio (E/Q) of ions ranging from 0.01 to 46.2 keV/q, while the TOF spectrometer determines mass-percharge ratio (M/Q) of ions from 1 to 64 amu/q. Using a forward modeling method detailed in Wang et al. (2024a, 2024b), the JADE-I data are fitted to get ion parameters, including abundances of different ions, plasma density, temperature, and 3-D bulk velocity. This study utilizes the data set described in Wang et al. (2024c), which is developed using this forward model. This data set consists of 70,487 good fits between 10 and 50 Jupiter radii (R_J) and covers Juno's orbits from PJ5 to PJ56, labeling the orbits by perijove (e.g., orbit insertion is PJ0).

Energetic particles are measured by JEDI (Jupiter Energetic Particle Detector Instrument) (Mauk et al., 2017), which consists of three nearly identical sensors. It uses solid-state detectors to measure ions, covering energies from 20 keV for protons and 150 keV for heavy ions up to over 1 MeV. Employing the TOF technique, the measurements distinguish three ion species: protons, helium, and heavies (primarily sulfur and oxygen). The partial density and pressure of each species are derived from the integral moments of the flux spectra using a method similar to that of Mauk et al. (2004). These values, including both protons and heavy ions, are then combined to obtain the energetic particle density and pressure. The uncertainty in the integral moments is typically less than 15%. This study uses the JEDI moments data set from PJ5 to PJ24, which is the latest available.

Since JADE and JEDI complement each other in energy range, combining their data sets is necessary to obtain reasonable plasma parameters. Finally, magnetic field data measured by the MAG instrument (Connerney et al., 2017) at 1-min resolution, spanning PJ5 to PJ56, are used to complement the plasma analysis.

2.2. Interchange Stability/Instability Criteria

Three flux tube integrals are required to evaluate the system's instability: flux tube volume (V), content (N), and entropy (S). They are defined as:

$$V = \int dl/B$$

$$N = \int n \cdot dl/B$$

$$S = p_0 V^{\gamma}$$
(1)

where d*l* is elemental length along the B-field line, *B* is the B-field magnitude, *n* is plasma number density, and p_0 is the flux tube averaged pressure. The adiabatic index is given by $\gamma = 5/3$.

Based on the integrals, Southwood and Kivelson (1987) developed a formalism to examine interchange instability in a planetary magnetosphere. The general stability criterion requires the following condition:

$$\frac{K}{V^{7}} \frac{\partial S}{\partial x_{p}} - \frac{mg_{e}}{V} \frac{\partial N}{\partial x_{p}} < 0 \tag{2}$$

where x_p is the interchange motion direction and m is the average ion mass in the plasma disk, assumed to be 24 amu. The effective gravity, g_e , is defined as:

$$g_e = r\Omega^2 - g \tag{3}$$

where Ω is Jupiter's angular velocity and r is the radial coordinate. The parameter g denotes Jupiter's gravity. The parameter K is defined as:

WANG ET AL. 4 of 11

$$K = \left[2(B^2/\mu_0)\kappa + nmg \right] / P_{\gamma} \tag{4}$$

where $P_{\gamma} = \gamma p_0 + B^2/\mu_0$ and $\kappa = (\vec{b} \cdot \vec{\nabla} \vec{b}) \cdot \vec{e_x}$ is the B-field curvature in the x_p direction, where \vec{b} and $\vec{e_x}$ are the unit vectors along B-field line and x_p , respectively. The profile of κ at different M-shells is presented in Supporting Information S1. μ_0 is vacuum permeability.

This study focuses on the radial interchange motion at the magnetic equator. Defining x_p as the positive radial direction, κ is negative, resulting in a negative K since the first term in Equation 4 dominates. The size of interchange motion is defined as Δx_p , with ΔS and ΔN as the changes in flux tube entropy and content over Δx_p , respectively. Following the same conversion of Eqn. 2 as in Wing et al. (2022), the total stability parameter (T_S) is defined as:

$$T_S = E_t + G_t \tag{5}$$

where $E_t = V^{-\gamma} \Delta S$ is the entropy term and $G_t = -K^{-1} \left(m g_e / V \right) \Delta N$ is the effective gravity term. A positive T_S (equivalent to Equation 2, noting that K is negative) indicates that the entropy term dominates the system, resulting in stability for interchange motion. In contrast, a negative T_S suggests an unstable system due to the dominance of the effective gravity term.

3. Results

3.1. Data Overview

Figure 2 shows an overview of the JADE forward modeling fits (panel (a)), JEDI numerical moments (panel (b)), and B-field data (panel (d)). The data are binned in the 2-D JMAG coordinate system that aligns the z-axis with Jupiter's magnetic dipole axis (see Fig. 34 in Bagenal et al. (2017)). Only plasma density, plasma pressure, and B-field magnitude are displayed, as these quantities are necessary for calculating the flux tube integrals. As Juno's orbit precesses southward gradually, data coverage becomes asymmetric: the northern side is mainly sampled in the post-midnight sector during the prime mission (to PJ34), while the southern side is better covered in the pre-midnight sector during the extended mission (Wang et al., 2024d). Therefore, the utilized JEDI moments (to PJ24) have a gap south of the equator.

The value shown for each bin is the median of all observations within that bin. Bins shown in gray either contain fewer than 10 data points or are measured in fewer than three orbits, making them statistically unreliable and therefore excluded from calculations. Panel (c) shows the total plasma density and pressure, obtained by summing JADE fits and JEDI moments only in bins that are well observed by both instruments. In general, both density and pressure decrease rapidly with increasing radial distance and away from the equator. The B-field is minimized at the magnetic equator due to the current sheet (panel (d2)).

3.2. Flux Tube Integrals and Interchange Stability/Instability

Based on Equation 1, the flux tube volume (V), content (N), and entropy (S) are obtained via numerical integration along the flux tube. The path of integration is calculated based on the JRM09 (Connerney et al., 2018) and CON2020 (Connerney et al., 2020) models through the Jupiter magnetic field community codes (Wilson et al., 2023), which produce a 3-D flux tube geometry due to the inclusion of B_{ϕ} (i.e., the azimuthal component) from the radial current. This geometry is transformed into a 2-D one in the ρ and z coordinates, where $\rho = \sqrt{x^2 + y^2}$. At each point along the path, the plasma and B-field parameters are calculated using 2-D interpolation, then V and N are computed by integrating over the path. S is calculated using V and P_0 , which is the average of all pressure values along the path.

As illustrated in Figure 2 panel (b), the JEDI moments primarily cover the northern side within $20 R_J$. To avoid under-sampling, integrations are performed only for the northern side with z > 0. Then the results are doubled to get the total flux tube integrals. In addition, the analysis is restricted to M-shells between 13 and 40, where the data sets provide sufficient coverage.

WANG ET AL. 5 of 11

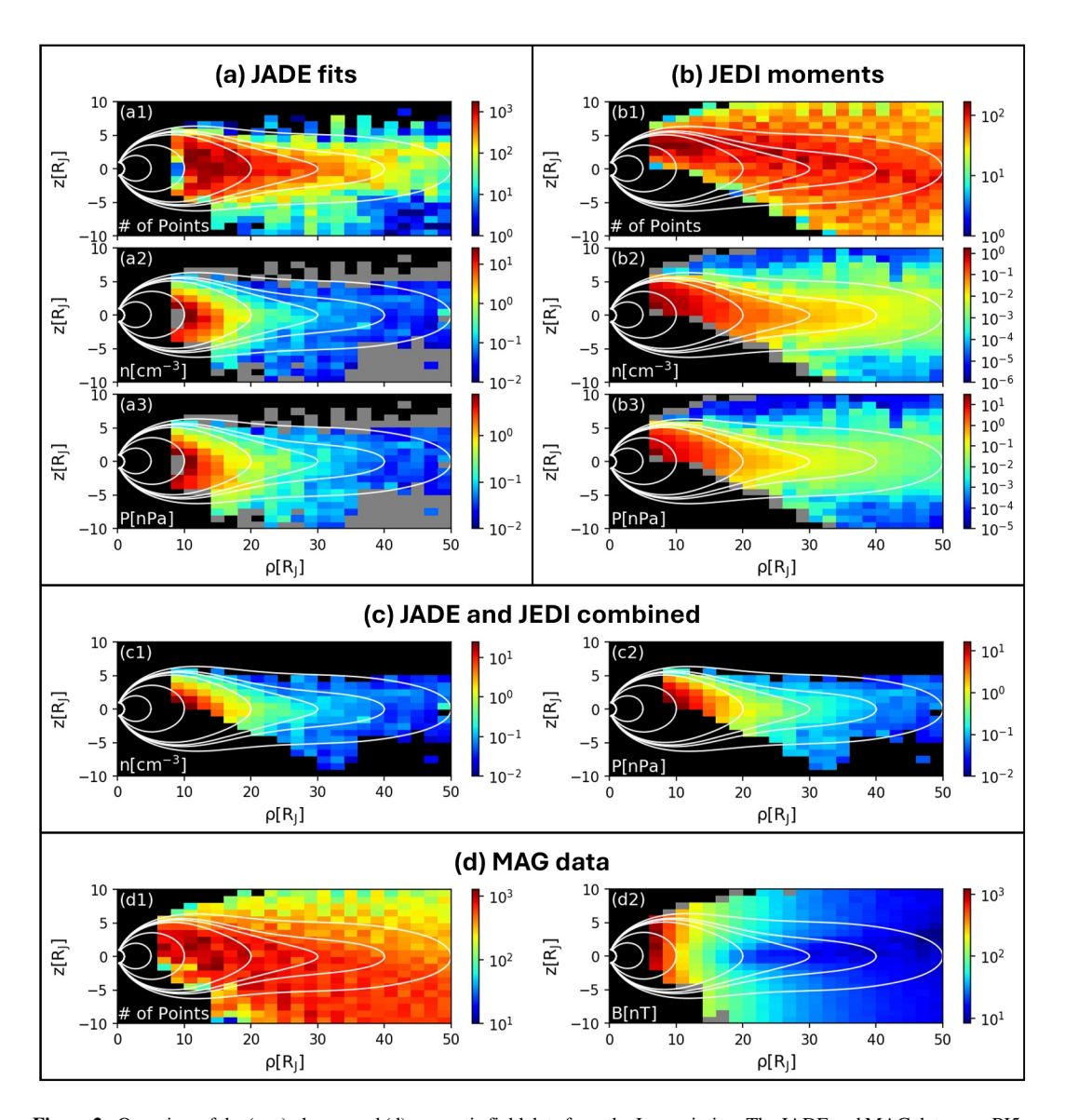


Figure 2. Overview of the (a–c) plasma and (d) magnetic field data from the Juno mission. The JADE and MAG data span PJ5 to PJ56, while the JEDI data span PJ5 to PJ24. Multiple species are included to determine the plasma density and pressure. The data are binned in the 2-D JMAG coordinate system with a bin size of $2 R_J \times 1 R_J$ and the value in each bin is the median.

Figure 3 shows the profiles of flux tube integrals. From M-shell 13 to 40, flux tube volume increases by over an order of magnitude (panel (a)). Flux tube content (N) decreases within M-shell 27 but increases beyond it (panel (b)). This increase is likely unrealistic and may result from a combination of factors, such as limitations in the B-field model or omission of regions where the density was too low to be measured. The general decreasing trend in N suggests an unstable system with respect to interchange motion. In contrast, flux tube entropy (S) increases with M-shell (panel (c)), indicating a stable system. These contradictory trends emphasize the necessity of using the Southwood and Kivelson (1987) criteria, which consider both quantities simultaneously.

As shown in Figure 2, reliable plasma parameters are not available yet near the polar region, meaning that the calculated integrals are partial. However, the missing contributions are minor. First, the integrals are line integrals of the unit flux area (i.e., $dA \sim 1/B$) along B-field lines. As the magnetic field strength increases, other parameters remain largely unchanged or decrease from the equator toward the poles. Hence, the polar region contributes minimally to the integrals. Second, for the analyzed M-shells, high-quality plasma data are available

WANG ET AL. 6 of 11

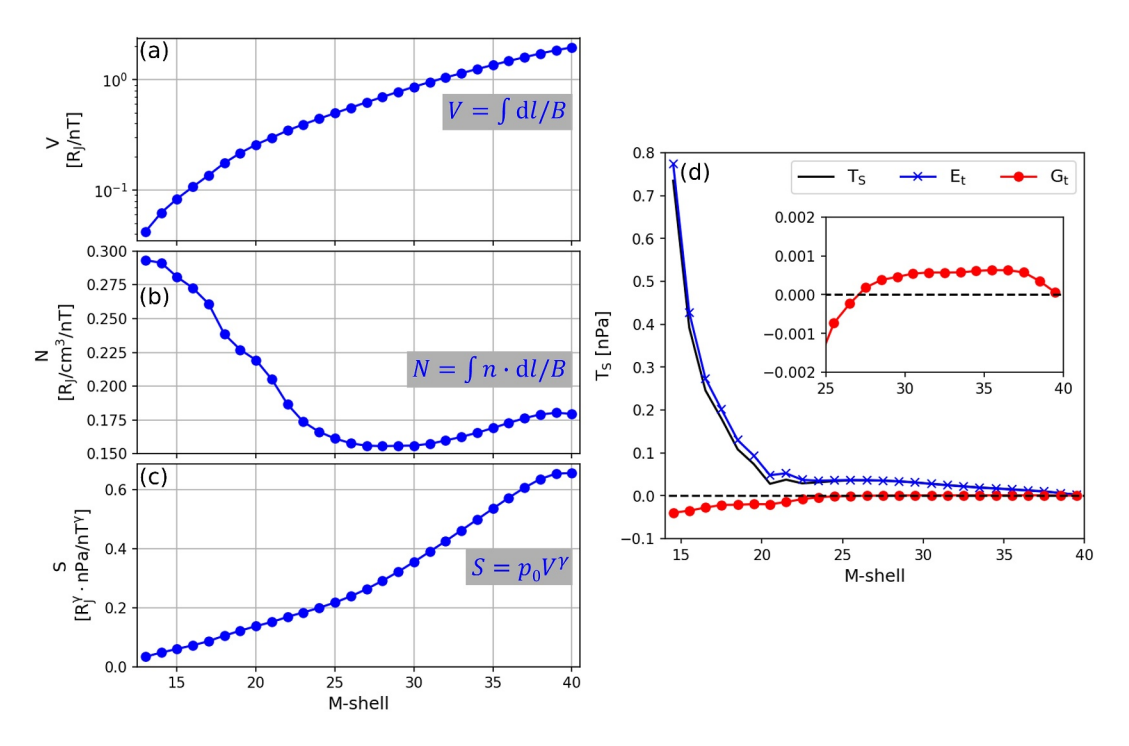


Figure 3. Flux tube integrals and interchange instability analysis at different M-shells in Jupiter's magnetosphere. (a–c) Flux tube volume (V), content (N), and entropy (S) integrated along the M-shells. (d) Total stability parameter (T_S) , entropy term (E_I) , and effective gravity term (G_I) .

at least within $4 R_J$ of the equator, matching the plasma disk's scale height (Bagenal & Delamere, 2011), thus capturing most of the plasma content in each flux tube in the calculations.

Finally, we analyze the interchange instability using the Southwood and Kivelson (1987) criteria, as shown in panel (d) of Figure 3. In the analysis, we choose the radial interchange distance to be $\Delta x_p = 1$ R_J. Inside M-shell 27, the effective gravity term (G_t) ranges from 5% to 42% of the entropy term (E_t), with an opposite sign, illustrating their competing effects: G_t destabilizes the system, whereas E_t stabilizes it. Beyond M-shell 27, however, both G_t and E_t are positive, indicating that they act in the same direction in controlling interchange instability. In conclusion, the total stability parameter (T_s) is positive and the entropy term dominates across all M-shells between 13 and 40, indicating that the system is, on average, stable against interchange motion when accounting for the combined effects of G_t and E_t . This average stability is expected; otherwise, the magnetodisc structure would not be maintained.

These conclusions are also similar to the statistical survey of Saturn's magnetosphere (Ma et al., 2024; Wing et al., 2022, 2024). The plasma production rate from Io at Jupiter (260–1,400 kg/s) greatly exceeds that from Enceladus at Saturn (12–250 kg/s), leading to a steeper flux tube content gradient and suggesting greater instability at Jupiter. Conversely, at Saturn, the higher neutral density and weaker heating processes reduce energetic particle pressure relative to thermal plasma (see Fig. 6 in Bagenal and Delamere (2011)). Because energetic particles help stabilize the system through entropy, this implies greater instability at Saturn. Future statistical studies are needed to assess whether Saturn's magnetosphere is more or less unstable than Jupiter's.

3.3. Case Study on Plasma Injection Event

To investigate why dynamic phenomena occur in a generally stable Jovian magnetosphere, we analyze a plasma injection event, following the approaches in Wing et al. (2022, 2024). An overview of this event is shown in Figure 4. This injection event occurred at 16.9 R_J on the inbound leg of PJ30. Juno traversed the plasma disk from south to north, as indicated by the reversal of B_r from negative to positive. The two blue regions represent outward moving ($u_r > 0$) cold, dense plasma, corresponding to ambient plasma. The middle red region represents inward moving ($u_r < 0$) hot, tenuous plasma. Combining the time-energy dispersion signature observed in panel (a), this region is identified as the injection event. During planetward injection, the plasma's angular velocity increases to

WANG ET AL. 7 of 11

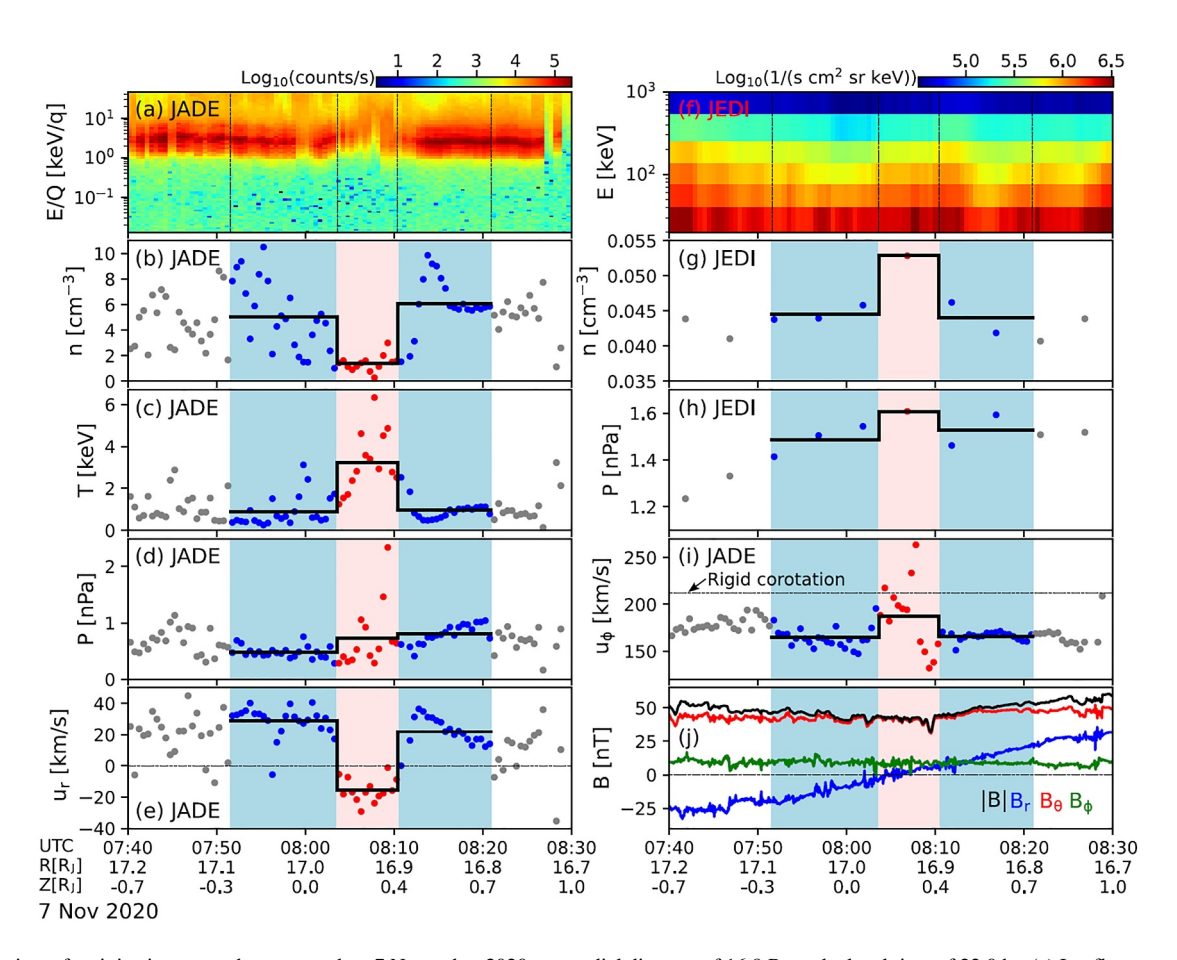


Figure 4. Overview of an injection event that occurred on 7 November 2020, at a radial distance of 16.9 R_J and a local time of 22.0 hr. (a) Ion flux spectra, (b) plasma density, (c) temperature, (d) pressure, (e) radial velocity, and (i) azimuthal velocity derived from the JADE measurements. (f) Ion flux spectra, (g) plasma density, and (h) pressure derived from the JEDI measurements. (j) Magnetic field data from the MAG measurements. In the related panels, the middle red region represents the injection event, with two blue regions as the ambient plasma. The horizontal black segments represent the average plasma parameters in the region.

conserve angular momentum. Consequently, the flux tube is accelerated in the azimuthal direction, generating super-corotating flows (panel (i)) (Wang, Bagenal, Wilson, Delamere, Cao, et al., 2025).

We assume that the injection and ambient plasmas occupy two distinct flux tubes adjacent to each other in the azimuthal direction. To determine flux tube integrals for each region, a normalization factor is calculated as the ratio of the local value in the region to the average equatorial value at the same radial distance from Figure 2. Then this factor is used to extrapolate plasma pressure and density along the field line, allowing for flux tube integral calculations. To calculate the total stability parameter T_S in Equation 5, the differences in flux tube entropy and content are defined as $\Delta S = S_{in} - S_{out}$ and $\Delta N = N_{in} - N_{out}$, where S_{in} and N_{in} represent the flux tube integrals for the injection event region, and S_{out} and N_{out} correspond to the average values in the ambient plasma regions surrounding the injection event. According to Wing et al. (2022, 2024), $T_S > 0$ suggests outward motion of the flux tube, while $T_S < 0$ indicates inward motion. In this event, $T_S = -0.82$ nPa, with $E_t = 0.15$ nPa and $G_t = -0.97$ nPa. Thus, applying the Wing et al. (2022, 2024) criteria suggests an inward moving flux tube, which aligns with observations of the injection event, where an inflow velocity of $u_r = -15$ km/s is obtained from forward modeling. Compared with the statistical average of $T_S = 0.24$ nPa at 17 R_J from Figure 2, the negative T_S observed during the injection event implies a violation of the stability criterion, leading to flux circulation and dynamic behavior.

Note that the applications of T_S in Sections 3.2 and 3.3 are different. When examining the average condition (Section 3.2), the sign of T_S serves as an indicator of whether the overall magnetosphere is stable. In contrast, when analyzing an injection event (Section 3.3), which is a perturbation to the ambient plasma, Wing et al. (2022, 2024) considered separately the leading and trailing edges of the injection flux tube, which have entropy gradients with the opposite signs. The sign of T_S indicates the direction of flux tube motion (see Fig. 2 in Wing et al. (2024)).

WANG ET AL. 8 of 11



4. Discussion

There are some caveats that are worth noting in this study, although they are minor and do not alter the conclusions. First, the derivations in Southwood and Kivelson (1987) assume an isotropic plasma. However, anisotropy can develop during instabilities (Paranicas et al., 1991). Liu et al. (2024) reported an average anisotropy ratio $(p_{\parallel}/p_{\perp}-1)$ below 20% within 40 R_J, indicating relatively weak anisotropic forces. McNutt et al. (1987) also reported an extreme ratio of 2.1, which may explain the plasma dropout due to ballooning motion during the Voyager era. Further work is needed to incorporate anisotropy into interchange criteria. Second, electron pressure is neglected in this analysis. As shown in Fig. 7d of Liu et al. (2024), electron pressure is lower than that of heavy ions, accounting for 20–30% of the heavy ion pressure at most. Additionally, including electron pressure would increase the flux tube entropy without affecting flux tube content, making the system more stable against interchange motions.

Third, JEDI cannot measure oxygen and sulfur ions below 150 keV, resulting in a pressure gap between 46 keV (the upper limit of JADE) and 150 keV. We compare the JEDI pressure with the Galileo/EPD results from Mauk et al. (2004), which covers energies above 50 keV (see the Supporting Information S1). The results suggest that JEDI could underestimate energetic particle pressure. Including this missing pressure would increase the total pressure and entropy, making the system more stable to interchange motion. Fourth, Jupiter's plasma disk exhibits significant temporal variations, for example, the orbit-by-orbit fluctuations. The calculated integrals are based on averaged conditions over multiple years, and short-term variations are not considered. Fifth, the adiabatic index is given by $\gamma = 1 + 2/f$. For monatomic, diatomic, and triatomic molecules, f = 3, 5, and 6, respectively. Outside 10 R_J , the plasma is primarily composed of oxygen and sulfur ions, so we assume f = 3 and f = 5/3 in this study. However, anisotropy with a larger parallel temperature could increase the adiabatic index f = 3 (see Fig. 2 in Livadiotis and Nicolaou (2021)). A larger f = 3 would lead to higher flux tube entropy, making the system more stable overall. Finally, Juno's observations of the plasma disk are limited to local times near midnight. Magnetopause effects and potential dayside/nightside differences are not included in the analysis.

5. Conclusions

The off-equatorial region of Jupiter's magnetosphere has been well observed by the Juno mission, providing high-quality plasma data and a valuable opportunity to investigate flux tube properties through in situ measurements. By utilizing accumulated data over multiple years, we analyze the system's instability from the perspective of flux tube interchange motion. Focusing on the middle magnetosphere, between M-shells 13 and 40, we draw the following key conclusions:

- 1. Flux tube volume increases by more than an order of magnitude with increasing radial distance.
- As radial distance increases, flux tube content decreases, destabilizing the system, while flux tube entropy increases, stabilizing the system.
- 3. On average, the entropy term dominates the system and the system is stable against interchange motion based on the criteria from Southwood and Kivelson (1987).
- 4. In the case study of an injection event, the prediction from the criterion aligns with the observed flow direction, indicating that the instability criterion can be locally violated.

In future studies, we plan to identify more flux tube interchange events observed by Juno and perform statistical analyses to improve our understanding of the dynamics in the Jovian magnetosphere.

Conflict of Interest

The authors declare no conflicts of interest relevant to this study.

Data Availability Statement

The plasma parameters from Juno/JADE are available from Wang et al. (2024). The Juno magnetometer data are Level 3, Version 01, from Connerney (2022), and the Juno/JEDI data are Level 3, Version 01, from Mauk (2024), both available on the NASA Planetary Data System.

WANG ET AL. 9 of 11



Acknowledgments

This work was supported at the University of Colorado as a part of NASA's Juno mission funded by NASA through contract 699050X with the Southwest Research Institute

References

- Abraham-Shrauner, B. (1967). Propagation of hydromagnetic waves through an anisotropic plasma. *Journal of Plasma Physics*, 1(3), 361–378. https://doi.org/10.1017/s0022377800003354
- André, N., & Ferrière, K. (2004). Low-frequency waves and instabilities in stratified, gyrotropic, multicomponent plasmas: Theory and application to plasma transport in the IO torus. *Journal of Geophysical Research*, 109(A12). https://doi.org/10.1029/2004ja010599
- André, N., & Lemaire, J. (2006). Convective instabilities in the plasmasphere. *Journal of Atmospheric and Solar-Terrestrial Physics*, 68(2), 213–227. https://doi.org/10.1016/j.jastp.2005.10.013
- Azari, A. R., Liemohn, M. W., Jia, X., Thomsen, M. F., Mitchell, D. G., Sergis, N., et al. (2018). Interchange injections at Saturn: Statistical survey of energetic H+ sudden flux intensifications. *Journal of Geophysical Research: Space Physics*, 123(6), 4692–4711. https://doi.org/10.1029/2018ja025391
- Bagenal, F., Adriani, A., Allegrini, F., Bolton, S., Bonfond, B., Bunce, E., et al. (2017). Magnetospheric science objectives of the Juno mission. Space Science Reviews, 213(1–4), 219–287. https://doi.org/10.1007/s11214-014-0036-8
- Bagenal, F., & Delamere, P. A. (2011). Flow of mass and energy in the magnetospheres of Jupiter and Saturn. *Journal of Geophysical Research*, 116(A5). https://doi.org/10.1029/2010ja016294
- Bagenal, F., & Dols, V. (2020). The space environment of IO and Europa. *Journal of Geophysical Research: Space Physics*, 125(5), e2019JA027485. https://doi.org/10.1029/2019ja027485
- Birn, J., Hesse, M., Schindler, K., & Zaharia, S. (2009). Role of entropy in magnetotail dynamics. *Journal of Geophysical Research*, 114(A9). https://doi.org/10.1029/2008ja014015
- Bolton, S., Thorne, R., Gurnett, D., Kurth, W., & Williams, D. (1997). Enhanced whistler-mode emissions: Signatures of interchange motion in the io torus. *Geophysical Research Letters*, 24(17), 2123–2126. https://doi.org/10.1029/97gl02020
- Connerney, J. (2022). Juno mag calibrated data j v1.0, jno-j-3-fgm-cal-v1.0 [Dataset]. NASA Planetary Data System. https://doi.org/10.17189/1519711
- Connerney, J., Benn, M., Bjarno, J., Denver, T., Espley, J., Jorgensen, J., et al. (2017). The Juno magnetic field investigation. Space Science Reviews, 213(1-4), 39–138. https://doi.org/10.1007/s11214-017-0334-z
- Connerney, J., Kotsiaros, S., Oliversen, R., Espley, J., Joergensen, J. L., Joergensen, P., et al. (2018). A new model of Jupiter's magnetic field from Juno's first nine orbits. *Geophysical Research Letters*, 45(6), 2590–2596. https://doi.org/10.1002/2018gl077312
- Connerney, J., Timmins, S., Herceg, M., & Joergensen, J. (2020). A Jovian magnetodisc model for the Juno era. *Journal of Geophysical Research:* Space Physics, 125(10), e2020JA028138. https://doi.org/10.1029/2020ja028138
- Delamere, P. A., Otto, A., Ma, X., Bagenal, F., & Wilson, R. J. (2015). Magnetic flux circulation in the rotationally driven giant magnetospheres. Journal of Geophysical Research: Space Physics, 120(6), 4229–4245. https://doi.org/10.1002/2015ja021036
- Goertz, C. (1983). Detached plasma in Saturn's front side magnetosphere. Geophysical Research Letters, 10(6), 455–458. https://doi.org/10.1029/gl010i006p00455
- Gold, T. (1959). Motions in the magnetosphere of the Earth. *Journal of Geophysical Research*, 64(9), 1219–1224. https://doi.org/10.1029/jz064i009p01219
- Hill, T. (1976). Interchange stability of a rapidly rotating magnetosphere. *Planetary and Space Science*, 24(12), 1151–1154. https://doi.org/10.1016/0032-0633(76)90152-5
- Johnson, J. R., & Wing, S. (2009). Northward interplanetary magnetic field plasma sheet entropies. *Journal of Geophysical Research*, 114(A9). https://doi.org/10.1029/2008ja014017
- Kivelson, M., Khurana, K., Russell, C., & Walker, R. (1997). Intermittent short-duration magnetic field anomalies in the io torus: Evidence for plasma interchange? Geophysical Research Letters, 24(17), 2127–2130. https://doi.org/10.1029/97g102202
- Kivelson, M., & Southwood, D. (2005). Dynamical consequences of two modes of centrifugal instability in Jupiter's outer magnetosphere. Journal of Geophysical Research, 110(A12). https://doi.org/10.1029/2005ja011176
- Liu, Z.-Y., Blanc, M., André, N., Bagenal, F., Wilson, R. J., Allegrini, F., et al. (2024). Juno observations of Jupiter's magnetodisk plasma: Implications for equilibrium and dynamics. *Journal of Geophysical Research: Space Physics*, 129(11), e2024JA032976. https://doi.org/10.1029/2024ja032976
- Livadiotis, G., & Nicolaou, G. (2021). Relationship between polytropic index and temperature anisotropy in space plasmas. *The Astrophysical Journal*, 909(2), 127, https://doi.org/10.3847/1538-4357/abda44
- Louarn, P., Andre, N., Jackman, C. M., Kasahara, S., Kronberg, E. A., & Vogt, M. F. (2015). Magnetic reconnection and associated transient phenomena within the magnetospheres of Jupiter and Saturn. Space Science Reviews, 187(1–4), 181–227. https://doi.org/10.1007/s11214-014-0047-5
- Ma, X., Delamere, P., & Otto, A. (2016). Plasma transport driven by the Rayleigh-Taylor instability. *Journal of Geophysical Research: Space Physics*, 121(6), 5260–5271. https://doi.org/10.1002/2015ja022122
- Ma, X., Delamere, P. A., Thomsen, M. F., Otto, A., Neupane, B., Burkholder, B., & Nykyri, K. (2019). Flux tube entropy and specific entropy in Saturn's magnetosphere. *Journal of Geophysical Research: Space Physics*, 124(3), 1593–1611. https://doi.org/10.1029/2018ja026150
- Ma, X., Wing, S., Delamere, P., Allen, R., Wilson, R., Burkholder, B., & Neupane, B. (2024). Statistical survey of magnetic flux integral quantities in Saturn's magnetosphere. *AGU fall meeting abstracts*, 2024, SM53B–2889.
- Mauk, B. (2024). Jedi calibrated (CDR) data jno j jed 3 cdr v1.0 [Dataset]. NASA Planetary Data System. https://doi.org/10.17189/1519713
- Mauk, B., Haggerty, D., Jaskulek, S., Schlemm, C., Brown, L., Cooper, S., et al. (2017). The Jupiter energetic particle detector instrument (JEDI) investigation for the Juno mission. Space Science Reviews, 213(1–4), 289–346. https://doi.org/10.1007/s11214-013-0025-3
- Mauk, B., McEntire, R., Williams, D., Lagg, A., Roelof, E., Krimigis, S., et al. (1998). Galileo-measured depletion of near-IO hot ring current plasmas since the voyager epoch. *Journal of Geophysical Research*, 103(A3), 4715–4722. https://doi.org/10.1029/97ja02343
- Mauk, B., Mitchell, D., McEntire, R., Paranicas, C., Roelof, E., Williams, D., et al. (2004). Energetic ion characteristics and neutral gas interactions in Jupiter's magnetosphere. *Journal of Geophysical Research*, 109(A9). https://doi.org/10.1029/2003ja010270
- Mauk, B., Saur, J., Mitchell, D., Roelof, E., Brandt, P., Armstrong, T., et al. (2005). Energetic particle injections in Saturn's magnetosphere. Geophysical Research Letters, 32(14). https://doi.org/10.1029/2005gl022485
- McComas, D., Alexander, N., Allegrini, F., Bagenal, F., Beebe, C., Clark, G., et al. (2017). The Jovian auroral distributions experiment (JADE) on the Juno mission to Jupiter. *Space Science Reviews*, 213(1–4), 547–643. https://doi.org/10.1007/s11214-013-9990-9
- McNutt, R., Belcher, J., & Bridge, H. (1981). Positive ion observations in the middle magnetosphere of Jupiter. *Journal of Geophysical Research*, 86(A10), 8319–8342. https://doi.org/10.1029/ja086ia10p08319
- McNutt, R., Coppi, P., Selesnick, R., & Coppi, B. (1987). Plasma depletions in the Jovian magnetosphere: Evidence of transport and solar wind interaction. *Journal of Geophysical Research*, 92(A5), 4377–4398. https://doi.org/10.1029/ja092ia05p04377

WANG ET AL. 10 of 11



- Paranicas, C., Mauk, B., & Krimigis, S. (1991). Pressure anisotropy and radial stress balance in the Jovian neutral sheet. *Journal of Geophysical Research*, 96(A12), 21135–21140. https://doi.org/10.1029/91ja01647
- Russell, C., Kivelson, M., & Khurana, K. (2005). Statistics of depleted flux tubes in the Jovian magnetosphere. *Planetary and Space Science*, 53(9), 937–943. https://doi.org/10.1016/j.pss.2005.04.007
- Scudder, J., Sittler Jr, E., & Bridge, H. (1981). A survey of the plasma electron environment of Jupiter: A view from voyager. *Journal of Geophysical Research*, 86(A10), 8157–8179. https://doi.org/10.1029/ja086ia10p08157
- Sittler, E., Andre, N., Blanc, M., Burger, M., Johnson, R., Coates, A., et al. (2008). Ion and neutral sources and sinks within Saturn's inner magnetosphere: Cassini results. *Planetary and Space Science*, 56(1), 3–18. https://doi.org/10.1016/j.pss.2007.06.006
- Sittler, E., & Strobel, D. F. (1987). Io plasma torus electrons: Voyager 1. Journal of Geophysical Research, 92(A6), 5741–5762. https://doi.org/10.1029/ja092ia06p05741
- Sittler, E., Thomsen, M., Johnson, R., Hartle, R., Burger, M., Chornay, D., et al. (2006). Cassini observations of Saturn's inner plasmasphere: Saturn orbit insertion results. *Planetary and Space Science*, 54(12), 1197–1210. https://doi.org/10.1016/j.pss.2006.05.038
- Southwood, D. J., & Kivelson, M. G. (1987). Magnetospheric interchange instability. *Journal of Geophysical Research*, 92(A1), 109–116. https://doi.org/10.1029/ja092ja01p00109
- Thorne, R., Armstrong, T., Stone, S., Williams, D., McEntire, R., Bolton, S., et al. (1997). Galileo evidence for rapid interchange transport in the IO torus. *Geophysical Research Letters*, 24(17), 2131–2134. https://doi.org/10.1029/97gl01788
- Vasyliunas, V. M. (1983). Plasma distribution and flow. Physics of the Jovian magnetosphere, 1, 395–453. https://doi.org/10.1017/cbo9780511564574.013
- Vogt, M. F., Kivelson, M. G., Khurana, K. K., Walker, R. J., Ashour-Abdalla, M., & Bunce, E. J. (2014). Simulating the effect of centrifugal forces in Jupiter's magnetosphere. *Journal of Geophysical Research: Space Physics*, 119(3), 1925–1950. https://doi.org/10.1002/2013ja019381
- Wang, J., Bagenal, F., Wilson, R., Valek, P., Ebert, R., & Allegrini, F. (2024). Juno/JADE ion parameters in Jupiter's magnetosphere between 10-50 RJ [Dataset]. Zenodo. https://doi.org/10.5281/zenodo.12802043
- Wang, J., Bagenal, F., Wilson, R. J., Delamere, P. A., Cao, X., Nerney, E., et al. (2025). Super-corotating flows in plasma disk within 30 Jupiter radii. Geophysical Research Letters, 52(3), e2024GL112910. https://doi.org/10.1029/2024gl112910
- Wang, J., Bagenal, F., Wilson, R. J., Delamere, P. A., Ebert, R. W., Valek, P. W., et al. (2025). Survey of cold plasma blobs in Jupiter's magnetosphere: Evidence for centrifugal instabilities. *Journal of Geophysical Research: Planets*, 130(7), e2025JE009021. https://doi.org/10.1029/2025je009021
- Wang, J., Bagenal, F., Wilson, R. J., Nerney, E., Crary, F., Dols, V., et al. (2024a). Forward modeling of 3-D ion properties in Jupiter's magnetosphere using Juno/Jade-I data. *Journal of Geophysical Research: Space Physics*, 129(4), e2023JA032218. https://doi.org/10.1029/ 2023ja032218
- Wang, J., Bagenal, F., Wilson, R. J., Nerney, E., Ebert, R. W., Valek, P. W., & Allegrini, F. (2024b). Radial and vertical structures of plasma disk in Jupiter's middle magnetosphere. *Journal of Geophysical Research: Space Physics*, 129(7), e2024JA032715. https://doi.org/10.1029/2024JA032715
- Wang, J., Bagenal, F., Wilson, R. J., Nerney, E., Ebert, R. W., Valek, P. W., et al. (2024d). Dawn-dusk asymmetry of plasma flow in Jupiter's middle magnetosphere observed by Juno. *Geophysical Research Letters*, 51(19), e2024GL110209. https://doi.org/10.1029/2024gl110209
- Wang, J., Bagenal, F., Wilson, R. J., Valek, P. W., Ebert, R. W., & Allegrini, F. (2024c). Ion parameters dataset from Juno/Jade observations in Jupiter's magnetosphere between 10 and 50 RJ. *Journal of Geophysical Research: Space Physics*, 129(12), e2024JA033454. https://doi.org/10.1029/2024ja033454
- Wilson, R., Vogt, M., Provan, G., Kamran, A., James, M., Brennan, M., & Cowley, S. (2023). Internal and external Jovian magnetic fields: Community code to serve the magnetospheres of the outer planets community. *Space Science Reviews*, 219(1), 15. https://doi.org/10.1007/s11214-023-00961-3
- Wing, S., & Johnson, J. R. (2009). Substorm entropies. Journal of Geophysical Research, 114(A9). https://doi.org/10.1029/2008ja013989
- Wing, S., & Johnson, J. R. (2010). Introduction to special section on entropy properties and constraints related to space plasma transport. *Journal of Geophysical Research*, 115(A1). https://doi.org/10.1029/2009ja014911
- Wing, S., Johnson, J. R., Thomsen, M. F., & Ma, X. (2024). Evolution of the flux tube instability parameters in plasma injections at Saturnian magnetosphere. Frontiers in Astronomy and Space Sciences, 11, 1479907. https://doi.org/10.3389/fspas.2024.1479907
- Wing, S., Thomsen, M., Johnson, J., Mitchell, D., Allen, R., Ma, X., & Delamere, P. (2022). The roles of flux tube entropy and effective gravity in the inward plasma transport at Saturn. *The Astrophysical Journal*, 937(1), 42. https://doi.org/10.3847/1538-4357/ac85b2
- Woch, J., Krupp, N., Khurana, K., Kivelson, M., Roux, A., Perraut, S., et al. (1999). Plasma sheet dynamics in the Jovian magnetotail: Signatures for substorm-like processes? *Geophysical Research Letters*, 26(14), 2137–2140. https://doi.org/10.1029/1999g1900493
- Wolf, R., Wan, Y., Xing, X., Zhang, J.-C., & Sazykin, S. (2009). Entropy and plasma sheet transport. *Journal of Geophysical Research*, 114(A9). https://doi.org/10.1029/2009ja014044

WANG ET AL. 11 of 11